P2.12

TROPICAL FREQUENCY AND DISTRIBUTION OF LIGHTNING BASED ON 10 YEARS OF OBSERVATIONS FROM SPACE BY THE LIGHTNING IMAGING SENSOR (LIS)

Rachel Albrecht*
University of Maryland, College Park, Maryland

Steve Goodman
NOAA/NESDIS – NASA/GSFC, Greenbelt, Maryland

Dennis Buechler
University of Alabama in Huntsville, Huntsville, Alabama

Themis Chronis
Hellenic Center for Marine Research, Greece

1. INTRODUCTION

Since its inception in late 1997, the Tropical Rainfall Measuring Mission (TRMM) satellite has collected detailed measurements of convective cloud systems over the tropics. The Lightning Imaging Sensor (LIS) aboard TRMM measures total lightning (intracloud and cloud-to-ground) using an optical staring imager. This sensor identifies lightning activity by detecting changes in the brightness of clouds as they are illuminated by lightning electrical discharges (Christian et al. 1999). A range of spatial, spectral and temporal filters are used to associate these changes into lightning (Christian et al., 2000).

LIS has a 600 km X 600 km field of view with a spatial resolution between 3 km (at nadir) and 6 km (at limb) (Christian et al., 1994). Since TRMM travels with a velocity of 7 km s^{-1} relative to Earth's surface, LIS can monitor a position on the Earth for lightning activity for approximately 80 s. One flash in 80 s allows a minimum detectable flash (fl) rate of 0.7 fl min^{-1} (Cecil et al., 2005) and the detection efficiency is estimated to be about 85% (Boccippio et al., 2002). The 35° inclination of TRMM orbit implies that locations near the equator are observed less frequently than the higher 35° latitude. This low-earth-orbiting feature requires a minimum period of 49 days for LIS instrument to observe most locations on Earth at least once in each local solar hour of the diurnal cycle (Boccippio et al., 1998; Boccippio et al., 2000).

Due to the low frequency of observations near the equator, total lightning climatology studies using LIS and the Optical Transient Detector were done with a horizontal grid resolution of 2.5 or 0.5 degrees (Boccippio et al., 2000; Nesbitt et al, 2000; Williams et al., 2000; Christian et al., 2003; Cecil, et al., 2005; Petersen et al., 2005; Cecil, 2006). Among these studies, Boccippio et al. (2000) analyzed the regional differences in tropical lightning distributions, addressing the differences between land and ocean and various geographic regions. Christian et al. (2003) generated lightning climatology maps based on 5 years of OTD total lightning measurements. These authors studied the geographical and seasonal distribution of lightning activity for the globe, pointing out the greatest flash density areas.

Nowadays, LIS has collected lightning measurements for over 10 years. In this study, we constructed climatology maps for the tropical region based on 10 years (1998-2007) of LIS total lightning data. As 10 years of measurements correspond to a considerable sample of earth's electrical activity over the equator, we constructed climatology maps over the tropics using a higher horizontal resolution. In section 2 we detail the data processing, and in section 3 we present the climatology maps, the main regional differences, and the flash lightning maximum ranking around the tropics.

2. METHODOLOGY

LIS raw data are a list of charged coupled device (CCD) events caused by optical pulses. Over these optical pulses, changes in the neutral oxygen emission line at 777.4 nm are monitored, corresponding to the strongest emission features in the cloud top optical spectra. Several spatial, spectral and temporal filters algorithms are used to geolocate the events, remove noise (Boccippio et al., 2002), and organize the remaining events into flashes by a clustering algorithm (Christian et al., 2000). In this study, a horizontal spatial resolution of 0.25°X0.25° is used, where the view time and

* *Corresponding author address*: Rachel I. Albrecht, Cooperative Institute for Climate Studies (CICS), NOAA/ESSIC, University of Maryland, College Park, MD 20740, e-mail: rachela@umd.edu.

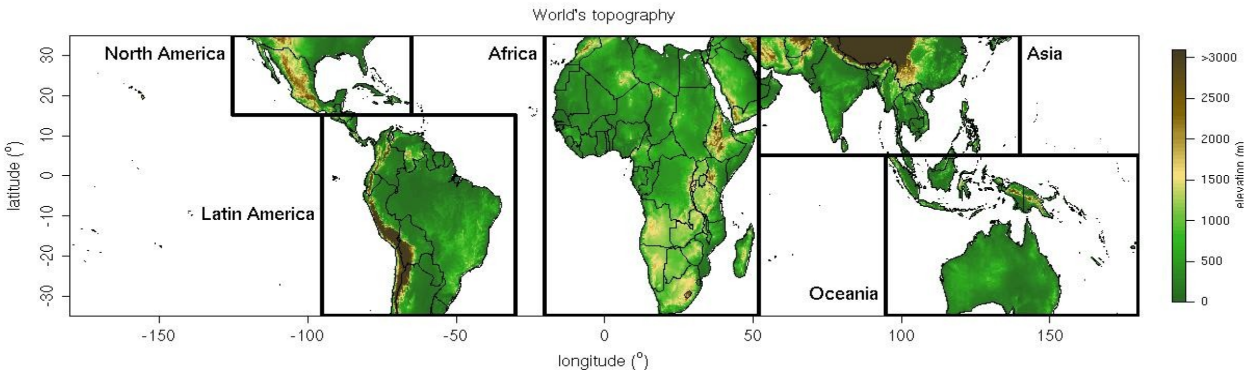

Figure 1 – World's topography from National Geophysical Data Center (NGDC/NOAA), and the rectangle delimitations of the five regions studied here.

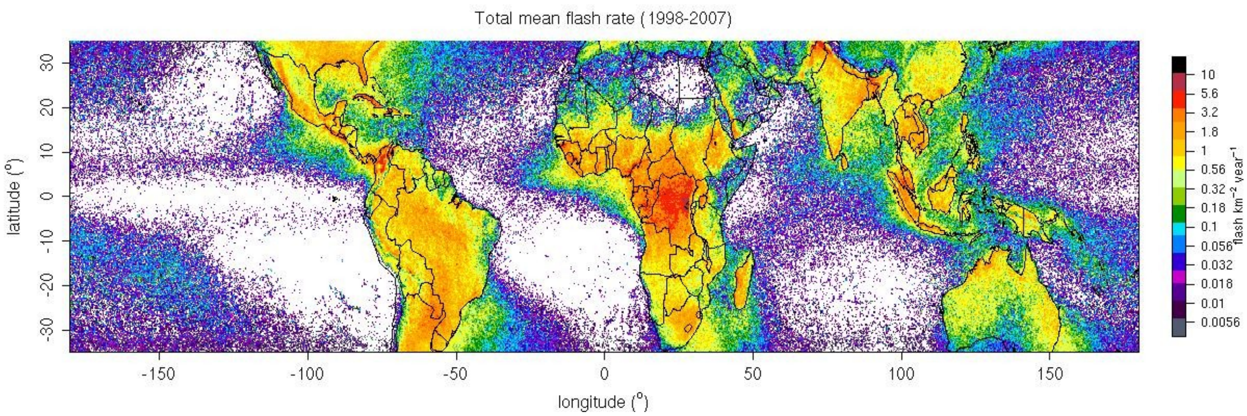

Figure 2 – Distribution of total lightning activity from 1998 to 2007.

number of flashes for each orbit are computed.

The mean lightning flash rate climatology maps are generated by a cumulative method, i. e. the ratio between the sum of all flashes and total view time for each horizontal grid point of analyzed periods. It is presented here mean total lightning flash rate climatology maps for all 10 years and for each season (DJF, MAM, JJA, SON). A ranking system of the 10 highest flash densities for 5 continental regions is also presented, based on the highest grid point in a 1ºx1º area. The continental regions are divided into rectangles that comprehends most of the world's tropical continents/landmasses: North America, Latin America, Africa, Asia and Oceania, as shown in Figure 1. Each ranked region is associated to the nearest city at the GEOnet Names Server (GNS) (National Geospatial-Inteligence Agency – NGA, 2008).

3. RESULTS

3.1 *Global features*

Figure 2 shows the mean total flash rate climatology observed by LIS from 1998 to 2007 in the 0.25ºX0.25º horizontal resolution grid. The basic difference between land and ocean can be clearly observed from Figure 2: deep convection (associated to lightning production) occurs more frequently over continental than oceanic environments (Mohr and Zipser, 1996; Nesbitt et al., 2000). However, some coast-oceanic regions presented flash rates from 0.55 to 1.0 flash km^{-2} year^{-1}. These regions are associated to frequent synoptic scale extratropical cyclones and cold fronts (such as south-southeast coasts of Brazil, South Africa and Australia) and large-scale convergence zones (such as the South Atlantic Convergence Zone, the South Pacific Convergence Zone, and the Intertropical Convergence Zone).

The highest flash rate of the planet has 17.43 flash km^{-2} year^{-1} in total mean lightning flash rate, and is located over the Maracaibo Lake in Venezuela [9.625ºN, 71.875ºW]. The second world's lightning maximum, with 14.70 flash km^{-2} year^{-1}, is over Congo Basin, at Mitumba Mountain's foot [2.625ºS, 26.625ºE], near the city of Kinzanza, Democratic Republic of Congo. These new results differ from Christian et al. (2003), who found Mitumba Mountain's foot as the “hottest spot” and did not point Venezuela in their findings.

The distribution of total mean lightning activity over Lake Maracaibo and Mitumba Mountain regions are shown in details in Figures 3 and 4, respectively, and Figure 5 shows the cumulative frequency of total mean flash rate for these two regions. It can be seen from these three figures that the world's maximum flash rate (Maracaibo Lake, Venezuela – Figure 3) is very localized surrounded by a few grid points over 5.6 flash km^{-2} $year^{-1}$, while the second maximum (Kinzanza, Dem. Rep. Congo – Figure 4) has a much greater area of flash rates over 5.6. Moreover, 50% of Maracaibo lightning activity presents flashes rates over 0.55 flash km^{-2} $year^{-1}$ while 50% of Mitumba lightning activity presents rates greater than 2.0 flash km^{-2} $year^{-1}$. On the tail distribution of flash rates, i. e., greater than 5.6 flash km^{-2} $year^{-1}$, Congo has 13% of its grid points while Northwestern South America has only 4%. Maracaibo Lake localized maximum feature explains why this region wasn't found by Christian et al. (2003) on their analysis, once these author studied global lightning activity using a 0.5°x0.5° composing grid with a 2.5° spatial moving average operator.

Both first and second world's maximum flash rate are induced by complex topography. The Maracaibo Lake is located inside Andes Mountains, at their most north chain where Andes forms a fork of elevated terrain, up to ~3650 m of height (Figure 3). Negri et al. (2002) found an annual mean rainfall rate local maximum greater than 0.6 mm h^{-1} over Maracaibo Lake, with a diurnal cycle peak from 0200 to 0400 local time. Figure 6 shows the local solar hourly mean flash rate for Northwestern South America and Mitumba Mountain regions of Figures 3 and 4, respectively. The nocturnal maximum lighting activity is clearly seen from 2300 to 0400 local solar hours (0.27 to 0.32 flash km^{-2} $year^{-1}$), and a second maximum is found 1700-1800 (~0.25 flash km^{-2} $year^{-1}$). Actually, nocturnal thunderstorms over Maracaibo Lake are so frequent that their lightning activity is locally known as the “Lighthouse of Catatumbo”, a local river that ends southwest of Maracaibo Lake. The “Lighthouse of Catatumbo” was used as a guide by Caribbean navigators in colonial times (Codazzi, 1841) and mentioned in the *La Dragontea* (1598) poem from the Spanish poet Felix Lope De Vega. Nowadays, these frequent thunderstorms are known as “The Never-Ending Storm of Catatumbo” and are explored by the local Venezuelan tourism with night trips tours to observe the beautiful storms.

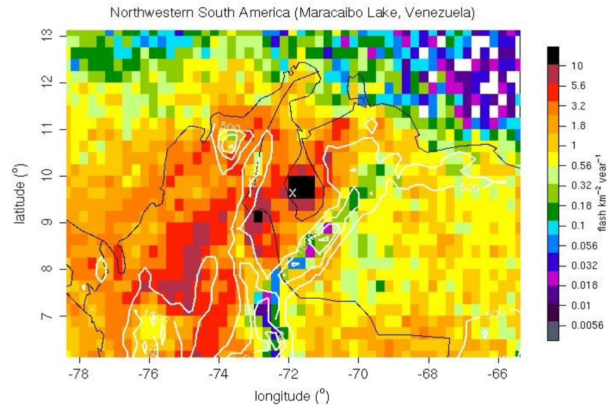

Figure 3 – Distribution of total lightning activity from 1998 to 2007 over Northwestern South America. Gray “x” indicates the *planet's first hot spot*, and the white lines indicate terrain elevation every 500 m.

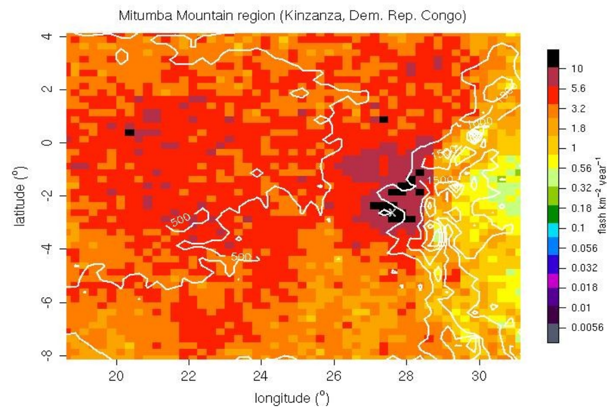

Figure 4 – Distribution of total lightning activity from 1998 to 2007 over Congo Basin Gray “x” indicates the *planet's second hot spot*, and the white lines indicate terrain elevation every 500 m.

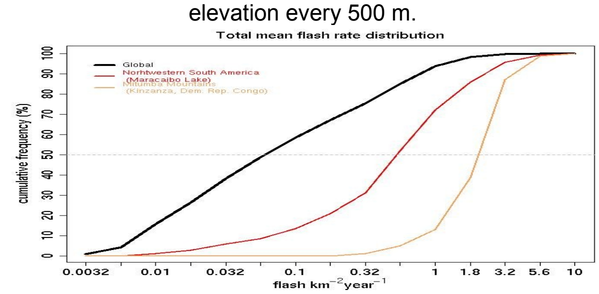

Figure 5 – Cumulative frequency distribution of total mean flash rate for the global region (Figure 2), Northwestern South America (Figure 3), and Mitumba Mountain (Figure 4).

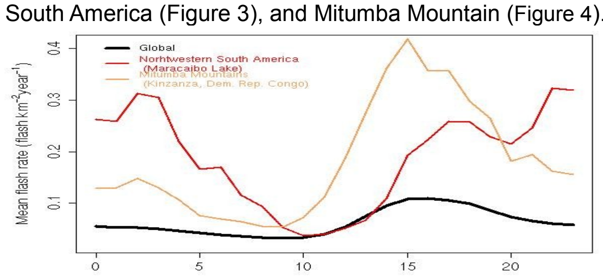

Figure 6 – Local solar hourly mean flash rate for the global region (Figure 2), Northwestern South America (Figure 3), and Mitumba Mountain (Figure 4).

Kinzanza's maximum flash rate is accompanied by high flash density (>5.6 flash km^{-2} $year^{-1}$) from 3.25ºS to 0.25ºN and from 26.00ºE to 28.75ºE, along the N-S Mitumba Mountain's west foot at the Democratic Republic of Congo, while the rest of Congo's Basin presents flashes rates >3.2 flash km^{-2} $year^{-1}$. Congo Basin is known for very deep convection (Boccippio et al., 2000; Nesbitt et al. 2000; Cecil et al. 2005) and has a peculiar difference in rainfall estimation from local rain gauges and satellites. McCollum et al. (2000) found that the Global Precipitation Climatology Project (GPCP) satellite estimates have approximately twice the magnitude of estimates produced from local rain gauges. These authors suggested that the rain gauges sample is not the problem and explained the discrepancy by unique local physical properties of air masses and cloud microphysics for such deep convection and low rainfall over this region: i) abundance of Saharan aerosols, resulting in abundance of cloud condensation nuclei, small drops and inefficient rain process; and ii) convective clouds forming under drier conditions, which in general have higher cloud base heights, that could increase the evaporation rate of falling rain. The moisture flux at Central Africa indicates a high westward transport from the Indian Ocean that is blocked by Mitumba Mountains east face in the lower levels (1000-865 mb), suggesting that convection at the west face of the mountains is initiated by a small but significant amount of eastward low-level moisture transport from Atlantic Ocean (McCollum et al., 2000). Drier and higher cloud base environments can also contribute to stronger in-cloud updrafts, which can also inhibit the warm cloud rain and enhance cold cloud rain, where the lightning is produced (Williams, et al. 2005; Carey et al., 2007; Albrecht et al., 2007). The lightning diurnal cycle of Figure 6 shows that thunderstorms over Congo Basin are driven by local solar heating, with a mean flash rate peak of 0.41 flash km^{-2} $year^{-1}$ at 1500 Solar Local Hour.

High elevated and complex terrain regions (Figure 1) over the tropics can be identified by low lighting activity in the mean total flash rate climatology map (Figure 2). For example, the South America's Andes can be seen by a 0.10-0.18 flash km^{-2} $year^{-1}$ line over its top from north Venezuela to south Chile, with medium electrical discharges of 0.56-1.8 flash km^{-2} $year^{-1}$ around its east foot. Mitumba Mountains in Congo Basin has relatively lower mean total flash rate densities (0.32-1.00 flash km^{-2} $year^{-1}$) than its west foot, and the Himalayas presents very low activity (0.1-1.8 flash km^{-2} $year^{-1}$) all around its north foot (China).

3.2 *Seasonal features*

Figure 7 shows the seasonal distribution of total lightning from 1998 to 2007. Northern and Southern hemispheric lightning activity follows season solar activity, with higher flash rates over continental regions of South America, Africa and Oceania in December-January-February (DJF),

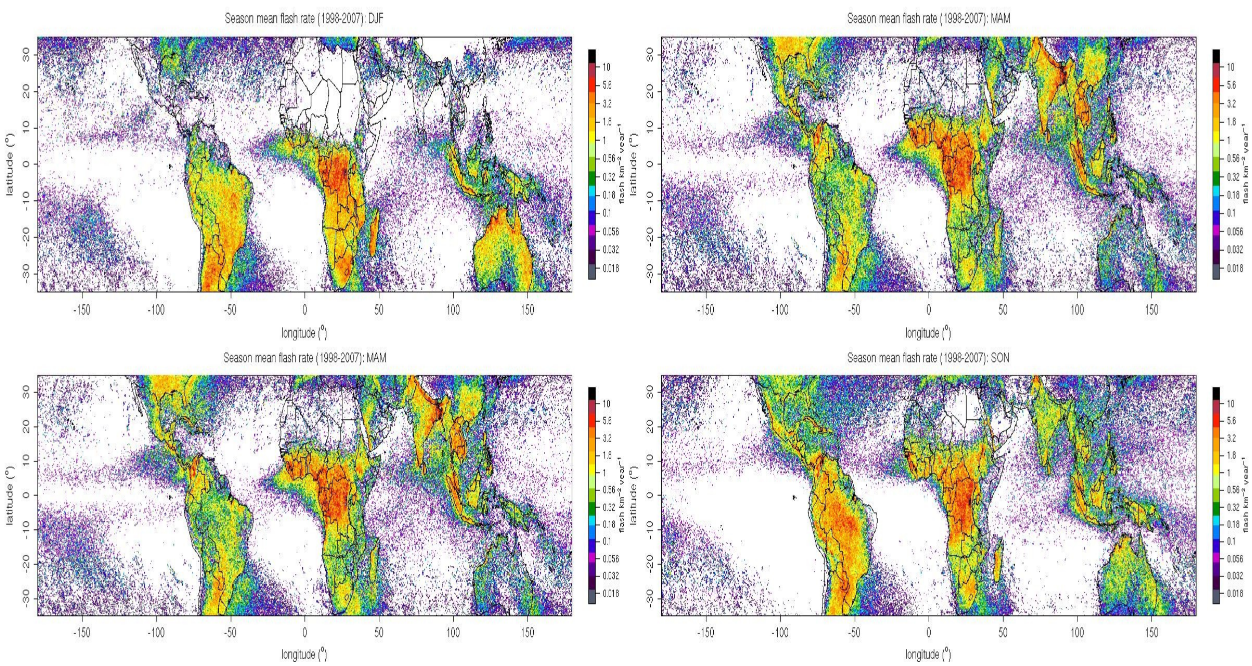

Figure 7 – Seasonal distribution of total lightning activity from 1998 to 2007.

Table 1 – Maximum and location of LIS total mean flash rate for each season from 1998 to 2007.

Season	Nearst location	Lat., Lon (°)	Flash rate (flash km^{-2} year^{-1})
DJF	Kinzanza, Dem Rep Congo	-2.625, 27.625	20.29
MAM	Sonamganj, Bangladesh	25.125, 91.375	24.35
JJA	Maracaibo Lake, Venezuela	9.625, -71.875	28.63
SON	Maracaibo Lake, Venezuela	9.625, -71.875	34.53

and higher flash rates over continental regions of North America and Asia in June-July-August (JJA).

The maximum flash rate during JJA is located at Maracaibo Lake, Venezuela (28.63 flash km-2 year-1), repeating this ranking again in September-October-November (SON – 34.53 flash km-2 year-1), as seen in Table 1. During DJF, the local maximum is located over the world's second lighting hot spot, Kinzanza, Dem. Rep. Congo. The maximum flash rate during March-April-May (MAM) is located at Sonamganj, Bangladesh, at the foot of Khasi Hills, Meghalaya, India, before the onset of Indian Monsoon.

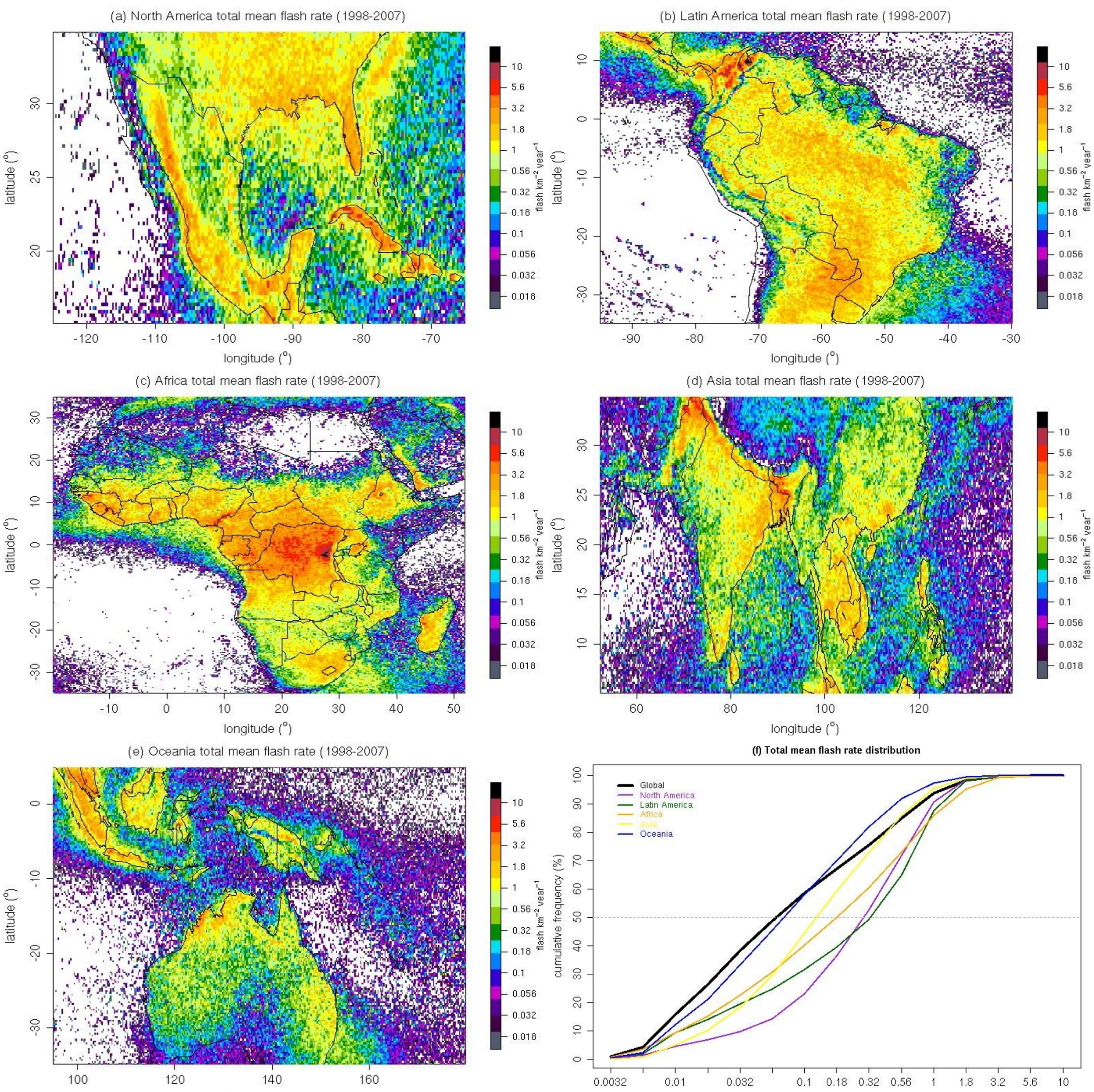

Figure 8 – Spatial distribution of total lightning activity from 1998 to 2007 for (a) North America, (b) Latin America, (c) Africa, (d) Asia and (e) Oceania. (f) Cumulative frequency distribution for the landmasses studied.

3.3 *Reginal features*

Spatial lightning flash rate distribution for the major tropical landmasses (North America, Latin America, Africa, Asia and Oceania – Figure 1) is presented in Figures 8a-e, while the cumulative frequency distribution of flash rates for these landmasses are presented in Figure 8f. Tables 2, 3, 4, 5 and 6 show the ranking of the ten highest flash rate locations for each one of the landmasses, respectively.

It can be seen from Figure 8 that North America and Latin America regions have most of their land with mean flash rates higher than 0.28 flash km^{-2} year^{-1} (50% and 47%, respectively), while Africa has a higher distribution of higher flash rates (over 28% of >0.56 flash km^{-2} year^{-1}). Asia and Oceania presented higher percentages of lower flash rates, with 50% of the lightning activity lower than 0.13 and 0.11 flash km^{-2} year^{-1}, respectively. The hot spots over North America (Table 2) are concentrated over Cuba and Haiti, with the first maximum at Finca Cocuyo [22.875ºN, 82.125ºW] having 7.59 flash km^{-2} year^{-1}. Note that North America's first place is less than half electrical active than world's hottest spot (Kinzanza, Dem. Rep. Congo, 17.43 flash km^{-2} year^{-1}). Mexico is in the 6th place, with 5.86 flash km^{-2} year^{-1} at Pedreira Segunda Seccion [17.625ºN, 93.625ºW] at the Sierra Madre del Sur's foot. Mexico was also ranked as the 8th and 9th highest flash density of this region, at Las Torres [22.375ºN, 105.375ºW] and Mesa Los Leales [26.375ºN, 107.875ºW], respectively, both east of the Sierra Madre del Norte. United States of America appears only in 10th place, with 5.07 flash km^{-2} year^{-1} at Orangetree, Florida.

Latin America highest flash rates are concentrated at Northwestern-Western South America and Central America, having 8 of the 10 ranking places (Table 3). The first one is, of course, the world's hottest spot, Maracaibo Lake, at Venezuela, 17.43 flash km^{-2} year^{-1}. The second city ranked is also in Venezuela, San Carlos, with 11.53 flash km^{-2} year^{-1}, while the 3rd, 4th and 6th place are over Colombia, at Andes' foot. Bolivia has the 5th Latin America highest flash density (6.59 flash km^{-2} year^{-1}), west of Andes' foot, while Argentina has the last two places (Estancia Noetinger-Lepetit – 5.27 flash km^{-2} year^{-1}, and Cancha Mercedes – 5.18 flash km^{-2} year^{-1}).

Africa has 8 of the 10 highest flash densities over the Congo Basin (Dem. Rep. Congo, Table 4). This landmass has the highest frequency of flash rates greater than 0.9 flash km^{-2} year^{-1}, that is 17%. Therefore, the 10th Africa's highest flash density (Kingombe, Dem. Rep. Congo) has 7.48 flash km^{-2} year^{-1}, comparable to North America hottest point (Finca Cocuyo, Cuba – 7.59 flash km^{-2} year^{-1}). Besides Congo Basin, Cameroon (east Africa), has the 6th and 8th

Table 2 – Maximums and locations of LIS total mean flash rate over North America.

Rank	Nearst location	Lat., Lon (°)	Flash rate (flash km^{-2} year^{-1})
1	Finca Cocuyo, Cuba	22.875, -82.125	7.59
2	Rio Seco, Cuba	22.375, -84.125	6.72
3	Savanette, Haiti	19.125, -72.125	6.29
4	Miranda, Cuba	20.375, -75.875	6.05
5	Conformidad, Cuba	22.875, -82.625	5.98
6	Pedr. Seg. Seccion, Mexico	17.625, -93.625	5.86
7	Bahia de Yara, Cuba	20.375, -77.125	5.84
8	Las Torres, Mexico	22.375, -105.375	5.81
9	Mesa Los Leales, Mexico	26.375, -107.875	5.45
10	Orangetree, Florida USA	26.375, -81.625	5.07

Table 3 – Maximums and locations of LIS total mean flash rate over Latin America.

Rank	Nearst location	Lat., Lon (°)	Flash rate (flash km^{-2} year^{-1})
1	Lake Maracaibo, Venezuela	9.625, -71.875	17.43
2	San Carlos, Venezuela	9.125, -72.875	11.56
3	El Garcero, Colombia	8.375, -74.625	10.48
4	Nuevo Horizonte, Colombia	8.875, -74.375	10.14
5	Finca La Primavera, Guatemala	14.375, -91.125	7.96
6	Labaredos, Colombia	5.375, -74.975	7.60
7	Quebrada La Union, Colombia	6.125, -75.625	7.25
8	Icuna, Bolivia	-17.125, -65.125	6.59
9	Estancia Noetinger-Lepetit, Arugentina	-27.125, -59.625	5.27
10	Cancha Mercedes, Argentina	-25.626, -57.875	5.18

Table 4 – Maximums and locations of LIS total mean flash rate over Africa.

Rank	Nearst location	Lat., Lon (°)	Flash rate (flash km^{-2} year^{-1})
1	Kinzanza, Dem. Rep. Congo	-2.625, 26.625	14.70
2	Kasindi, Dem. Rep. Congo	-1.625, 28.125	11.39
3	Bafwanenzeke, Dem. Rep. Congo	0.875, 27.375	11.34
4	Losofila, Dem. Rep. Congo	0.375, 30.375	10.98
5	Ifwafondo, Dem. Rep. Congo	1.625, 22.375	9.40
6	Agborkem, Cameroon	5.875, 9.125	8.47
7	Yongoli, Dem. Rep. Congo	-0.375, 22.625	8.46
8	Kentane, Camerron	6.625, 10.375	7.65
9	Wenge, Dem. Rep. Congo	-1.625, 20.875	7.61
10	Kingombe, Dem. Rep. Congo	-3.875, 26.625	7.48

Table 5 – Maximums and locations of LIS total mean flash rate over Asia.

Rank	Nearst location	Lat., Lon (°)	Flash rate (flash km^{-2} year^{-1})
1	Bharakh, India	33.125, 74.625	9.61
2	Dala Kandao, Pakistan	34.375, 72.375	9.60
3	Sonamganj, Bangladesh	25.125, 91.375	7.10
4	Tor Nao, Pakistan	33.875, 70.375	6.85
5	Langrial, Pakistan	33.875, 73.125	6.58
6	Nayakhel, Bangladesh	25.125, 92.125	6.54
7	Nagrota Khas, India	32.125, 76.375	6.52
8	Duddar, India	32.875, 75.125	6.35
9	Bilaur, India	32.625, 75.625	6.12
10	Moghulkhel, Afghanistan	33.625, 70.125	5.93

Table 6 – Maximums and locations of LIS total mean flash rate over Oceania region.

Rank	Nearst location	Lat., Lon (°)	Flash rate (flash km^{-2} year^{-1})
1	Kuala Lumpur, Malaysia	3.125, 101.625	7.46
2	Strait of Melacca, Malaysia/Indonesia	3.125, 100.625	6.44
3	Polori, Indonesia	3.625, 98.125	6.04
4	Bukit Berangan, Malaysia	1.625, 103.875	5.82
5	Depok Satu, Indonesia	-6.375, 106.875	5.47
6	Alur Kerok, Indonesia	4.375, 97.625	5.23
7	Mitchell Plateau, Australia	-14.975, 125.875	5.21
8	Mount York, Australia	-15.375, 125.375	4.99
9	Goobaieri Bay, Australia	-15.125, 129.875	4.94
10	Synott Creek, Australia	-16.375, 125.125	4.67

positions, with 8.47 and 7.65 flash km^{-2} year^{-1}, respectively, both west of Mount Cameroon.

Asia landmass has 8 of the 10 highest flash densities (9.61-5.93 flash km^{-2} year^{-1}) just south of Himalaya's foot (Table 5), at India (1st, 7th, 8th, and 9th), Pakistan (2nd and 5th) and Afghanistan (10th). The two other rank positions, 3rd and 6th, are located in Bangladesh south of Khasi Hills. Flash densities higher than 3.2 flash km^{-2} year^{-1} (5% - Figure 8f) are concentrated over Himalaya and Khasi Mountains foot.

Oceania highest flash rate densities (Table 6) are located over Malaysia, Indonesia and Australia. Kuala Lumpur, Malaysia, has the first place with 7.46 flash km^{-2} year^{-1}. As North America landmass, Oceania has its first flash rate ranking position comparable to Africa's last one (Table 4). This feature can be observed in Figures 8c, 8e and 8f, where Africa has 5% of its grid points with flash rates greater than 1.78 flash km^{-2} year^{-1}, while Oceania has only 0.8%. Most of the Indonesian and Malaysia maximums are located between the two islands and between Bukit Barisan and Titiwangsa Mountains. All Australian maximums (5.21-4.67 flash km^{-2} year^{-1}, 7-10th positions) are located around the North-Northeastern coast of the country, around Joseph Bonapart Gulf, dominated by local sea breeze convection.

The local diurnal cycle of mean flash rate landmasses studied here are presented in Figure 9. All landmasses present a lightning activity maximum from middle (1500) to late (1800) local solar afternoon hours. Africa has the highest mean flash density, 0.42 flash km^{-2} year^{-1}, at 1500 and

Asia has two maximums of ~0.8 flash km^{-2} year^{-1} at 1600 and 1900 local solar hour. Africa and Latin America presents higher nocturnal flash rate densities (~0.7 flash km^{-2} year^{-1} from 2300 to 0400 local solar hours), while Oceania has the lower nocturnal lightning activity (~0.4 flash km^{-2} year^{-1}).

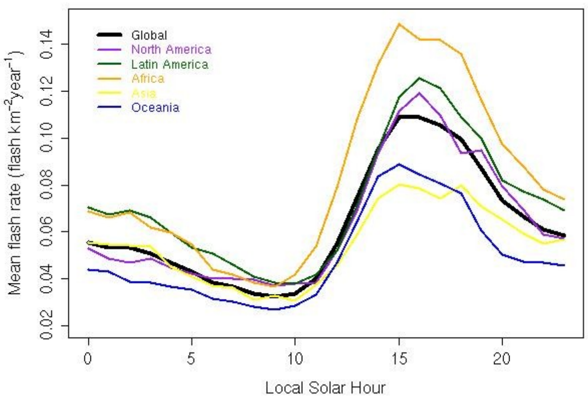

Figure 9 – Local solar hourly mean flash rate for North America (Figure 8a), Latin America (Figure 8b), Africa (Figure 8c), Asia (Figure 8d) and Oceania (Figure 8e) landmasses.

4. CONCLUSIONS

Data from 10 years of TRMM-LIS observations were used to generate higher resolution lightning climatology maps. This new climatology was able to identify more localized features of lightning activity over the tropics, and the world's maximum flash rate was found to be over Lake Maracaibo, Venezuela., leaving the earlier maximum at Mitumba Mountain foot (Christian et al., 2003) in the second place.

The main difference between land and ocean convection and lightning frequency could be inferred from this study. Over all continents, the main maximums were related to a complex topography, as Maracaibo Lake at North Andes' fork, Kinzanza at Mitumba's foot, Baraksh and many others at Himalaya's foot, Sierras Madre del Sur and Norte in Mexico, and Bukit Barisan Mountains in Indonesia. Further studies are needed to fully understand the physical mechanisms behind these regional lighting maximums.

REFERENCES

Albrecht, R. I., C. A. Morales, J. R. Neves, M. A. F. Silva Dias, 2007: Lightning activity on thunderstorms relative to the microphysics, thermodynamics and large-scale features in the Amazon region. *33rd Conf. Radar Meteor.*, Cairns, Australia, American Meteorological Society, paper 8A.3.

Boccippio, D. J., W. J. Koshak, and R. J. Blakeslee, 2002: Performance assessment of the Optical Transient Detector and Lightning Imaging Sensor. Part I: Predicted diurnal variability. *J. Atmos. Oceanic Thechnol.*, 19, 1318-1332.

Boccippio, D. J., S. J. Goodman, S. Heckman, 2000: Regional differences in tropical lightning distributions. *J. Appl. Meteor.*, 39, 2231-2248.

Boccippio, D. J., K. Driscoll, J. Hall, D. E. Buechler, 1998: *LIS/OTD Software Guide.* Global Hydrology and Climate Center, 142 pp.

Cecil, D. J, 2006: Global distributions of thunderstorms based on 7+ years of TRMM. *2nd Conf. on Meteor. App. of Lightning Data,* Altanta, GA, American Meteorological Society, paper 5.3.

Cecil, D. J., S. J. Goodman, D. J. Boccippio, E. J. Zipser, and S. W. Nesbitt, 2005: Three years of TRMM precipitation features. Part I: Radar, Radiometric, and Lightning characteristics. *Mon. Wea. Rev.*, 133, 543-566.

Carey, L., and K. Buffalo, 2007: Environmental control of cloud-to-ground lighting polarity in severe storms, *Mon. Wea. Rev.* , 135 , 1327-1353.

Christian, H. J., and co-authors, 2003: Global frequency and distribution of lightning as observed from space by the Optical Transient Detector. J. Geophys. Res., 108, 4005, doi:10.1029/2002JD002347.

Christian, H. J, R. J. Blakeslee, S. J. Goodman, D. M. Mach, 2000: *Algorithm Theoretical Basis Document (ATBD) for the Lightning Imaging Sensor (LIS)*, 53pp, NASA/Marshall Space Flight Center, Huntsville, AL.. (Available as http://eospso.gsfc.nasa.gov/eos_homepage/for_scientists/atbd/index.php, posted 1 Feb. 2000)

Christian, H. J, and co-authors, 1999: The Lightning Imaging Sensor. *Proc. 11th Int. Conference on Atmospheric Electricity*, Guntersville, AL, International Comission on Atmospheric Electricity, 746-749.

Codazzi, A., *Resúmen de la geografía de Venezuela, por Augustín Codazzil,* Paris, Impr. de H. Fournier y compia, 1841. (in Spanish)

McCollum, J. R., A. Grubber, and M. B. Ba, 2000: Discrepancy between gauges and satellite estimates of rainfall in Equatorial Africa. *J.*

Appl. Metor., 39, 666-679.
Mohr, K. I., and E. J. Zipser, 1996: Defining mesoscale convective systems by their 85 Ghzice-scattering signatures. *Bull. Amer. Meteor. Soc.*, 77, 1179-1189.
National Geospatial-Intelligence Agency – NGA, 2008: *GEOnet Names Server,* Complete Files of Geographic Names for Geopolitical Areas from GNS. (Available as http://earth-info.nga.mil/gns/html/geonames_dd_dms_date_20081223.zip, posted 23 Dec 2008).
Nesbitt, S. W., E. J. Zipser, D. J. Cecil, 2000: A census of precipitation features in the tropics using TRMM: Radar, ice scattering, and lightning observations. *J. Climate,* 13, 4087-4106.
Petersen, W. A., H. J. Christian, and Steven A. Rutledge, 2005: TRMM observations of the global relationship between ice water content and lightning. Geophys. Res. Lett., 32, L14819, doi:10.1029/2005GL023236.
Williams, E., V. Mushtak, D. Rosenfeld, S. Goodman, and D. Boccippio, 2005: Thermodynamic conditions favorable to superlative thunderstorm updraft, mixed phase microphysics and lightning flash rate, *Atm. Res.*, 76, 288-306.
Williams, E., K. Rothkin, D. Stevenson, D. Boccippio, 2000: Global lightning variations caused by changes in thunderstorm flash rate and by changes in the number of thunderstorms. *J. Appl. Meteor.*, 39, 2223-2230.